

## A dynamical simulated annealing approach to the electronic structure of liquid metals

This article has been downloaded from IOPscience. Please scroll down to see the full text article.

1990 J. Phys.: Condens. Matter 2 221

(<http://iopscience.iop.org/0953-8984/2/1/018>)

View [the table of contents for this issue](#), or go to the [journal homepage](#) for more

Download details:

IP Address: 171.66.16.96

The article was downloaded on 10/05/2010 at 21:23

Please note that [terms and conditions apply](#).

## A dynamical simulated annealing approach to the electronic structure of liquid metals

J Hafner<sup>†‡</sup> and M C Payne<sup>‡</sup>

<sup>†</sup> Cavendish Laboratory, University of Cambridge Madingley Road,  
Cambridge CB3 0HE, UK

<sup>‡</sup> Institut für Theoretische Physik, Technische Universität Wien,  
Wiedner Hauptstrasse 8/10, A 1040 Wien, Austria

Received 27 July 1989

**Abstract.** We present a dynamical simulated annealing approach to the self-consistent calculation of the electronic structure of liquid metals. Models for the atomic structure are generated using a classical microcanonical molecular dynamics simulation based on interatomic potentials derived from pseudopotential perturbation theory. The electronic structure is calculated by numerically integrating the dynamical simulated annealing equations of motion for the electron states at fixed atomic coordinates, using the same pseudopotential. Detailed results are presented for liquid Al, Si, Ge, As and Te. As far as experimental information is available, the calculated electronic density of states is in good agreement with the photoemission spectra. The dynamical simulated annealing calculations are compared with electronic structure calculations based on minimal basis sets such as the linear-muffin-tin-orbital method. We find that at comparable accuracy, the dynamical simulated annealing approach reduces the computational effort for 64-atom models by about a factor of ten. Compared to a full density-functional molecular-dynamics approach the present method achieves self-consistency between the atomic and the electronic structure only at the level of a linear-response approach. For good liquid metals such as Si the result of the present approach based on a combination of perturbation and *ab initio* methods leads to results equivalent to those based on full density-functional molecular-dynamics calculations, but it requires only about 1% of the computational effort. For molten materials close to a semiconductor/semimetal transition (liquid As and Te) covalent bonding effects however are expected to have a non-negligible influence on the electronic density of states at the Fermi level. Here the combination of the present approach with full density-functional MD calculations should help to get accurate results at a much lower computational effort.

### 1. Introduction

The self-consistent calculation of the electronic structure of topologically disordered (liquid or amorphous) materials remains a considerable challenge. The problem is that in order to account for the effect of the local fluctuations in the atomic arrangement on the electronic structure self-consistency should be achieved locally, at every atomic site. To date the only technique which is able to achieve self-consistency at a local level is the ‘supercell’ technique [1–3]. The electronic structure is calculated for atoms arranged in a periodically repeated ‘supercell’, using standard *k*-space techniques. The coordinates of the atoms within this cell are generated via molecular dynamics or Monte Carlo

calculations, based either on effective volume and pair forces derived from pseudopotential perturbation theory where it is applicable or on empirical pair potentials. A configuration average may be taken by repeating the electronic structure calculations for independent configurations along the simulated phase-space trajectory. Evidently this requires a very efficient technique for calculating the electronic states. Standard techniques for self-consistent electronic structure calculations proceeding by repeated diagonalisation of the Hamiltonian matrix become inefficient when the number of degrees of freedom (i.e. essentially the number of basis states necessary to represent the electronic wavefunctions in the cell) is large. A number of such calculations for liquid and amorphous metals and alloys have been performed using minimal-basis-set methods such as the linear-muffin-tin-orbital (LMTO) method in the atomic-sphere-approximation (ASA) [4], but these represent a major computational effort [1–3].

Recently an entirely new development was initiated by a seminal paper by Car and Parrinello [5]. Under the name of density-functional molecular-dynamics this paper introduced three important new ideas: (i) The solution of the one-electron Schrödinger equation can be performed in various ways. Car and Parrinello adopted a global minimisation of the total energy via a 'dynamical simulated annealing' (DSA) procedure based on a molecular dynamics algorithm. Any other efficient minimisation technique could be used as well. (ii) The use of a mixed real and reciprocal space representation leads to a very efficient scaling of the computational effort with the number of atoms in the supercell, or equivalently with the number  $N$  of basis functions. The basic step in any iterative matrix diagonalisation is the multiplication of some approximate eigenfunction  $\psi$  by a Hamiltonian  $H = T + V$ . Normally such an operation takes  $N^2$  steps. However multiplication with a diagonal matrix takes only  $N$  steps. If  $\psi$  is expanded in plane waves the operation  $T\psi$  can be performed as a diagonal multiplication in reciprocal space. The same applies for a local potential  $V$  if  $\psi$  is calculated on a real-space grid and the operation  $V \cdot \psi$  is performed in real space. The rate-limiting factor is then the fast Fourier transform between the two representations which takes  $N \log N$  steps. The challenge is to achieve a similar performance for non-local potentials. The dynamical simulated annealing approach based on (i) and (ii) allows to use very large plane-wave basis sets of the order of several  $10^3$  to  $10^4$  plane waves in electronic structure calculations. (iii) The third point is that convergence in the ionic equations of motion (EOM) and in the one-electron wave equations may be approached simultaneously. The DSA equations of motion for the electronic degrees of freedom and the Newtonian equations of motion of the ions (with the forces on the ions given by the Hellmann–Feynman theorem) together form the density-functional molecular-dynamics (DF MD) equations of motion of the coupled electron-ion system. The solution of these equations allows for a self-consistent calculation of the atomic and the electronic structure. However, even by present-day standards such a calculation represent a very large computational effort and allows to explore only a very small region of phase space, typical simulations runs being limited to about  $10^{-12}$  s.

In the present work we have exploited the DSA concept (i.e. (i) and (ii)) to perform accurate and efficient calculations of the electronic structure for a number of liquid elements, ranging from nearly-free-electron metals such as Al to liquid semimetals such as As and Te. The atomic configurations serving as the basis of these calculations have been generated using conventional molecular dynamics simulations based on volume- and pair forces derived from second-order pseudopotential perturbation theory. These simulations can be extended over much longer times, typically  $10^{-10}$  s. The same local pseudopotentials are used in the DSA calculations of the electronic structure and in the

molecular dynamics calculations of the atomic structure. Compared to a full density-functional molecular-dynamics calculation self-consistency of the atomic and the electronic structures is achieved only at the level of a linear response approach, but the comparison of the calculated atomic correlation functions and of the electronic density of states with experiment and with the available DF MD results show that very realistic results can be obtained in this way. The computer-time necessary for the calculation is comparable to that for a very few time steps of the DF MD, i.e. only a fraction of  $10^{-3}$  to  $10^{-2}$  of the computer-time for a fully converged DF MD calculation. We also compare our results with LMTO-supercell calculations and find a comparable accuracy at about one tenth of the computational effort.

## 2. Dynamical simulated annealing

Car and Parrinello [5] write the DSA equation of motion for the electronic state  $\psi_{nk}$  as

$$\mu \ddot{\psi}_{nk}(\mathbf{r}, t) = -\frac{\partial E}{\partial \psi_{nk}(\mathbf{r}, t)} + \sum_{nn'} \Lambda_{nn'}^k \psi_{n'k}(\mathbf{r}, t) \quad (1)$$

where  $E$  is the total energy,  $\Lambda_{nn'}^k$  are the Lagrangian multipliers for the constraints of orthogonality and normalisation, and  $\mu$  is a fictitious mass. Using a plane wave representation for the  $\psi_{nk}$  and removing the Lagrangian factors for the orthogonality constraint, the equation of motion (EOM) for the coefficient of the plane wave  $\exp[i(\mathbf{k} + \mathbf{G})\mathbf{r}]$  becomes (in atomic units,  $\hbar^2/2m = 1$ ,  $\Lambda_{nn}^k = \lambda_{nk}$ )

$$\mu \ddot{C}_{n,k+\mathbf{G}} = -[(\mathbf{k} + \mathbf{G})^2 + V_{\mathbf{G}=0} - \lambda_{nk}] C_{n,k+\mathbf{G}} - \sum_{\mathbf{G} \neq \mathbf{G}'} V_{\mathbf{G}-\mathbf{G}'} C_{n,k+\mathbf{G}'} \quad (2)$$

where  $V$  stands for the one-electron potential calculated in the density-functional approximation. The wavefunctions are orthogonalised after each integration step via a Gram-Schmidt procedure. Car and Parrinello used a second-order Verlet algorithm to integrate the EOM. Payne *et al* [6, 7] realised that because (2) is an oscillator equation with frequency  $\bar{\omega} = \{[(\mathbf{k} + \mathbf{G})^2 + V_{\mathbf{G}=0} - \lambda_{nk}]/\mu\}^{1/2}$  it can be integrated analytically. The analytic integration allows us to use a larger time step and gives faster convergence.

Calculations for metals entail special complications because of the Fermi surface. Crossing of levels close to the Fermi surface could lead to discontinuous changes in the  $C_{n,k+\mathbf{G}}$  and to instabilities in the EOM. We have adopted the following procedure to treat metals. The electronic eigenvalues  $\varepsilon_{n,k}$  are Gaussian-broadened. The superposition of the Gaussians defines a smooth electronic density of states (DOS) which is used for the determination of the Fermi level  $E_F$ . Integration of the Gaussians up to  $E_F$  defines an occupancy factor  $w(E_F - \varepsilon_{n,k})$  for each electron state which determines the weight with which this state contributes to the new charge density. In any case this procedure led to a fast convergence of the EOM.

The calculation of the charge density, total energy, DOS etc requires a sampling of the Brillouin zone of the 'supercell'. The calculations of Car and Parrinello [8] on a 54-atom supercell for liquid and amorphous Si use the  $\Gamma$  point ( $\mathbf{k} = 0$ ) and result in a rather strongly structured density of states. Conventional LMTO-supercell calculations [1–3] have demonstrated that a more extended Brillouin-zone sampling (up to ten  $\mathbf{k}$ -points on a regular grid in the irreducible part of the Brillouin zone of a 64-atom cell) or the use of the Chadi–Cohen special points [9] lead to a smoother and more accurate DOS. The use of the  $\Gamma$  point (or of any other single high-symmetry point) leads to a rather inaccurate

**Table 1.** Input data for the molecular dynamics calculation of the atomic structure and the dynamical simulated annealing calculation of the electronic structure: temperature  $T$ , number density  $n$ , and pseudopotential core radius  $R_c$ .

	$T$ (K)	$n$ ( $\text{\AA}^{-3}$ )	$R_c$ ( $\text{\AA}$ )
Al	965	0.05298	0.582
Si	1773	0.05553	0.520
Ge	1250	0.04430	0.529
As	1100	0.03900	0.534
Te	723	0.02710	0.545

result for the DOS because even for these rather large cells the  $\Gamma$ -point eigenvalues still show a rather high degree of near-degeneracy. The present calculations are based on a single Chadi-Cohen point ( $\mathbf{k} = (0.25, 0.25, 0.25)(2\pi/a)$ ) for a cubic cell with a cube edge  $a$ ) which gives a better representation of the DOS than the  $\Gamma$  point.

### 3. Electronic structure of liquid metals

#### 3.1. Atomic structure

In the following we describe in detail our calculations for liquid Al, Si, Ge, As and Te. The trend in the liquid structures of these elements has been studied recently in a series of publications [3, 10–13]. It has been shown that the transition from a close-packed, hard-sphere-like structure in l-Al to more open structures in the liquid elements from groups IV to VI of the Periodic Table may be understood in terms of the interplay of volume and pair forces and of the systematic variation of the pair potentials with electron density and pseudopotential. The variation of the pair potentials across the Periodic Table is well described even by calculations based on a simple empty-core pseudopotential, with the core radius  $R_c$  fitted to the electronic properties of the crystalline elements [13] (see Table XVIII in Cohen and Heine [14]). We remark at once that all our results are stable with respect to small changes (+5%) of  $R_c$ . The Ichimaru-Utsumi [15] form for the local-field corrections to the electron-gas screening function has been used in the calculation of the pair potentials. The input data for our calculations are summarised in table 1.

The atomic structure of the liquid has been calculated using classical microcanonical molecular dynamics, using a fourth-order predictor-corrector algorithm for the integration of the ionic EOM [10, 16]. Figure 1 shows the effective pair potential  $\Phi(R)$  and the pair correlation function  $g(R)$  for liquid Si. The experimental  $g(R)$  is compared with: (a) the MD-ensemble average for a 512-atom model (80 independent configurations out of a molecular dynamics trajectory of 3200 time steps with  $\Delta t = 4 \times 10^{-15}$  s, i.e.  $t = 1.28 \times 10^{-11}$  s), (b) the MD-ensemble average for a 64-atom model (800 independent configurations out of a simulation extending over 32 000 time steps,  $t = 1.28 \times 10^{-10}$  s), and (c) the  $g(R)$  calculated for a single 64-atom configuration serving as the basis for the DSA-calculations of the electronic DOS. We find that the full MD-average leads to a very good agreement with experiment [17]. Differences between the 512-atom and the 64-atom ensemble averages appear only for distance larger than the cube edge of the small cell ( $R > 10.5 \text{\AA}$ ), provided that the reduced number of atoms can be compensated

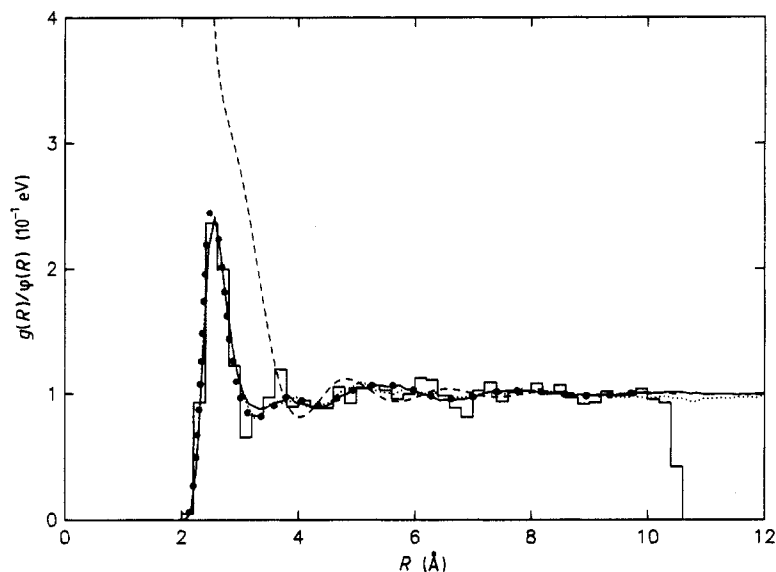


**Figure 1.** Interatomic pair potential  $\Phi(R)$  and pair correlation function  $g(R)$  for liquid silicon at  $T = 1170$  K. The broken curve shows the pair potential, shifted by +1. The full curve shows the pair correlation function calculated from an ensemble average for a 512-atom model, the dotted curve represents the result of a configuration average for a 64-atom model, and the histogram the  $g(R)$  calculated for a single 64-configuration. The full dots give the results of the experimental pair correlation function (after Gabathuler and Steeb [17]). Note that the results of the 512-atom and the 64-atom simulations differ significantly only for distances larger than the cube edge of the smaller cell (i.e.  $R > 10.5$  Å).

by a more extended ensemble average. Even a single 64-atom represents the characteristic aspects of the structure of liquid Si surprisingly well. Note that the calculated  $g(R)$  is in very good agreement with the result of the DF MD calculations for l-Si [8]. For a detailed discussion of the MD-simulations of l-Ge, As, and Te see [3, 10–12]. For l-As the present results based on the pair potentials calculated using perturbation theory are again well confirmed by full DF MD simulations [18]. Table 2 summarises the most relevant structural information—note that the low coordination numbers and the characteristic bond-angles of these elements are well described.

### 3.2. Electronic structure

The integration of the DSA-EOM (2) for the electronic states was performed using the analytic method of Payne *et al* [6, 7] for supercells containing 64 atoms. The energy cut-off determining the highest-energy plane-wave states was set at a minimum of 70 eV. Calculations for l-Al and l-Si using cut-off energies up to 160 eV showed that the form of the DOS is entirely unaffected by this relatively low cut-off value of 70 eV, the higher-energy plane-wave states merely lead to a small rigid shift of the DOS. The integration of the DSA-EOM was extended over 70 steps. After 50 steps the total energy is converged to five leading figures.

Figure 2 shows the DOS calculated for the same configuration of liquid Ge, using the DSA in a plane-wave basis as described here, and using a conventional LMTO-ASA supercell

**Table 2.** Coordination number  $N_c$ , interatomic distances  $R_i$  for the first and second coordination shell, and position  $\theta_{\max}$  of the main peak in the bond-angle distribution function: comparison of molecular dynamics simulation and experiment.

		$N_c$	$R_1$ (Å)	$R_2$ (Å)	$R_2/R_1$	$\theta_{\max}$ (deg)
Al	MD	10.9	2.69	4.89	1.82	58, 109
	exp. <sup>f</sup>	10.5	2.71	4.95	1.83	60, 90, 120 <sup>a</sup>
Si	MD	6.7	2.52	5.50	2.18	60, 90 <sup>b</sup>
	exp. <sup>g</sup>	6.4	2.45	5.50	2.24	109.5 <sup>c</sup>
Ge	MD	7.6	2.66	5.75	2.16	60, 90 <sup>b</sup>
	exp. <sup>g</sup>	6.5	2.65	5.73	2.16	109.5 <sup>c</sup>
As	MD	3.0	2.61	3.83	1.47	94
	exp. <sup>h</sup>	3.0	2.50	3.75	1.50	97 <sup>d</sup>
Te	MD	2.56	2.76	4.15	1.50	100
	exp. <sup>i</sup>	2.63	2.81	4.20	1.49	102 <sup>e</sup>

<sup>a</sup> Bond angle in face-centred cubic Al.

<sup>b</sup> Liquid Si and Ge show very diffuse bond-angle distributions with two very broad peaks.

<sup>c</sup> Bond-angle in the diamond structure of Si and Ge.

<sup>d</sup> Bond-angle in the rhombohedral structure of crystalline As.

<sup>e</sup> Bond-angle in the trigonal structure of crystalline Te.

<sup>f</sup> [25]

<sup>g</sup> [17].

<sup>h</sup> [19].

<sup>i</sup> [20].

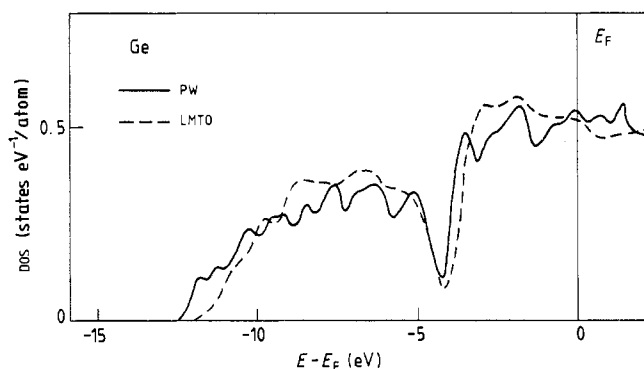


**Figure 2.** Comparison of the results of self-consistent calculations of the electronic density of states for a 64-atom configuration of liquid Ge, based on dynamical simulated annealing calculations in a plane-wave basis as described here (PW-full line) and based on linear-muffin-tin-orbital (LMTO) calculations in an atomic-sphere-approximation (dotted line, after [3] and [21]).

calculation [3, 20] (based on ten  $k$ -points on a regular grid in the Brillouin zone). The somewhat more pronounced fluctuations in the DOS obtained by DSA are due mainly to the fact that a single special point does not quite as well as a sampling over ten  $k$ -points, but otherwise the agreement between the LMTO-ASA and the DSA results is certainly very

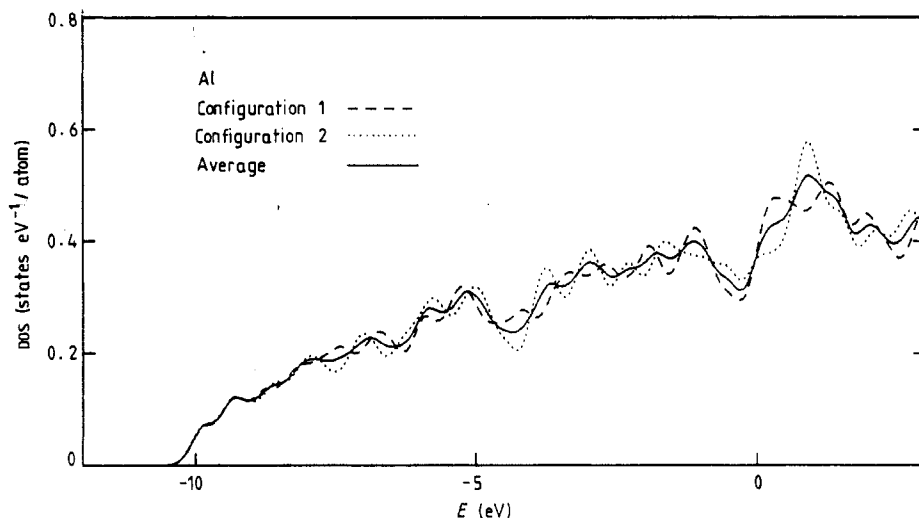


**Figure 3.** Electronic density of states for two independent 64-atom configurations of liquid Al (dotted and broken lines) and configuration average. See text.

encouraging. The important point is that for these 64-atom supercells the computer-time per  $k$ -point needed for the DSA calculations is about a factor of ten lower than for the LMTO calculations. The reduction of the computational effort will be even more important for larger cells as the computer-time for the LMTO scales with  $N^3$ , whereas for the DSA the scaling goes as  $N \log N$ . A certain drawback is the larger core memory required for the DSA calculations.

In principle one should always take a configuration average over a sufficient number of independent configurations. Figure 3 compares the DOS for two independent configurations of liquid Al, taken at an interval of 1000 time steps (i.e. at a time interval of  $4 \times 10^{-12}$  s) along the MD trajectory. We find the differences in the DOS to be rather small, especially near the bottom of the band. But even close to the Fermi level where they are larger, the differences are still of the order of magnitude of the uncertainty introduced by the restricted Brillouin zone sampling (or equivalently, by the small number of atoms in the supercell). Therefore the following calculations have been restricted to a single representative atomic configuration.

Figure 4 shows the electronic DOS for liquid Al, Si, Ge, As and Te. Only Al and Si show the nearly-free-electron like DOS that is often assumed to be characteristic for all s, p-bonded liquid metals. In Ge and As a deep pseudo-gap, and in l-Te a real gap splits the valence band into a lower part containing exactly two electrons per atom and an upper part that accommodates the remaining electrons. For l-Si the present results are in good agreement with the DF MD results of Car and Parrinello [8] (but see the comments concerning the spikiness of the DF MD DOS). The NFE-form of the DOS for l-Al and the existence of a pseudo-gap in the DOS of l-Ge are well confirmed by recent photoemission experiments [21] as is shown in figure 4. For l-Te (where no spectroscopic data for the melt are available) the calculated DOS agrees well with the photoemission spectrum of crystalline Te [22, 23] (see figure 4), as suggested by the similarity in the local order in liquid and crystalline Te (see table 2). The fact that the lower part of the band contains exactly two electrons suggest that the band is a pure s band and that the upper part of



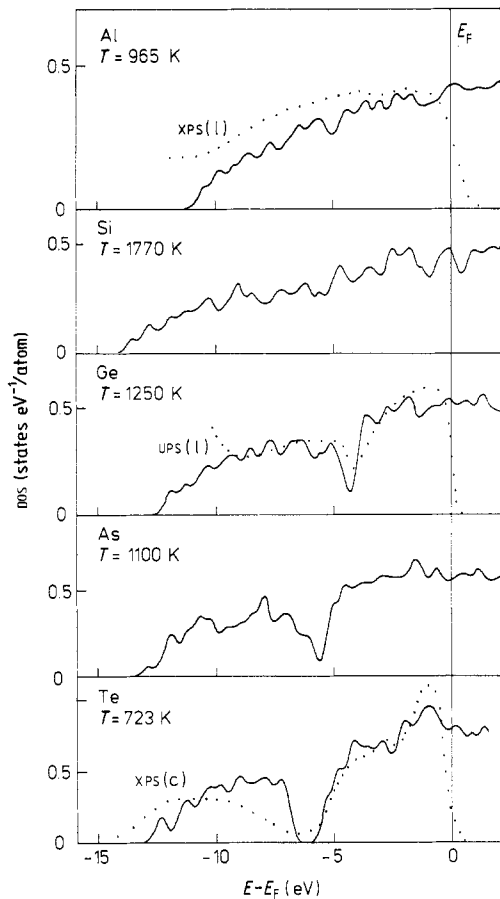


**Figure 4.** Electronic density of states for liquid Al, Si, Ge, As, and Te calculated by the dynamical simulated annealing approach (full lines). For Al and Ge the dotted lines show respectively the x-ray (xps) and ultraviolet (ups) photoemission spectra measured for the molten metal (after Indlekofer *et al* [22]). For Te we show for comparison the xps spectrum of the crystalline material (after [23] and [24]).

the is a p band. This is indeed confirmed by the angular-momentum decomposed DOS resulting from the LMTO ASA calculations [3, 21]. The origin of the pseudo-gap is two-fold: (a) due to the lower coordination number the overlap between orbitals centred at neighbouring atoms is no longer large enough to promote the strong s, p hybridisation necessary for the formation of a NFE-like valence band. (b) The separation of s and p states is enhanced in the heavier elements by relativistic effects which tend to bind s electrons more strongly than p electrons. In liquid Ge a third point is important: the 4s electrons partially penetrate the rather extended 3d core, so that the 4s electrons see a more attractive ionic potential. In our approach the relativistic effects and the effect of the core-penetration are taken into account by adjusting the core-radius to the empirical pseudopotentials.

The only open question concerns the DOS of l-As and l-Te at the Fermi-level. The present results suggest a metallic DOS at  $E_F$ . Crystalline As is a semimetal, crystalline Te a semiconductor with a very narrow band-gap. To decide whether covalent bonding effects not included in the pseudopotential perturbation calculation of the interatomic forces lead to the formation of a pseudo-gap at  $E_F$  in the liquid will require a full DF MD calculation. If the entire calculation starting from some arbitrary configuration is done within the DF MD framework this calculation will be by nearly a factor of  $10^3$  more time-consuming than the present calculation. Preliminary results suggest that if the DF MD

calculation is started from a configuration created in a classical simulation based on the effective pair potentials, a well converged result can be achieved at a much reduced effort.

#### 4. Conclusions

To conclude: we have shown that dynamical simulated annealing (DSA) calculations of the electronic structure of liquid metals and semimetals are as accurate, but computationally much more efficient than conventional supercell techniques based on iterative matrix diagonalisation. Compared to a full density-functional molecular-dynamics calculation the present approach achieves self-consistency between the atomic and the electronic structures only at the level of a linear-response approach but allow for a much more extended sampling of phase space. The comparison of our results with the DF MD results of Car and Parrinello [8] for l-Si and of Li *et al* [18] for l-As and with the experimental data (diffraction data and photoelectron spectroscopy) suggests that for Al, Si, Ge and perhaps As this is not a very serious restriction. Only for l-Te which is much closer to a semiconductor–semimetal transition a full calculation of the Hellmann–Feynman forces within a DF MD framework appears to be necessary. But even here the combination of the perturbation- and *ab initio* methods introduced here helps to define a reasonably realistic starting point for the DF MD simulations and to reduce the computational effort.

#### Acknowledgments

We would like to thank Professor V Heine for his encouragement and for a critical reading of the manuscript. JH acknowledges the hospitality of Clare College and the Cavendish Laboratory, Cambridge, where this work was performed with the financial assistance of the Royal Society and the Science and Engineering Research Council. MCP acknowledges financial support from the Royal Society.

#### References

- [1] Jaswal S S and Hafner J 1988 *Phys. Rev. B* **38** 7311  
Hafner J and Jaswal S S 1988 *Phys. Rev. B* **38** 7320
- [2] Hafner J and Jaswal S S, Tegze M, Pflugi A, Krieg J, Oelhafen P and Güntherodt H J 1988 *J. Phys. F: Met. Phys.* **18** 2583
- [3] Jank W and Hafner J 1988 *Europhys. Lett.* **7** 283
- [4] Skriver H 1984 *The LMTO Method* (Berlin: Springer)
- [5] Car R and Parrinello M 1985 *Phys. Rev. Lett.* **55** 2471
- [6] Payne M C, Joannopoulos J D, Allan D C, Teter M P and Vanderbilt D H 1986 *Phys. Rev. Lett.* **56** 2656
- [7] Payne M C, Bristowe P D and Joannopoulos J D 1987 *Phys. Rev. Lett.* **58** 1348
- [8] Car R and Parrinello M 1988 *Phys. Rev. Lett.* **60** 204
- [9] Chadi D J and Cohen M L 1973 *Phys. Rev. B* **8** 5747
- [10] Arnold A, Mauser N and Hafner J 1989 *J. Phys.: Condens. Matter* **1** 965
- [11] Hafner J 1989 *Phys. Rev. Lett.* **62** 748
- [12] Hafner J J. *Phys.: Condens. Matter* at press
- [13] Hafner J and Heine V 1983 *J. Phys. F: Met. Phys.* **13** 2479
- [14] Cohen M L and Heine V 1970 *Solid State Phys.* **24** 235 (New York: Academic)

- [15] Utsumi K and Ichimaru S 1980 *Phys. Rev. B* **24** 7385
- [16] Arnold A and Mauser N *Comput. Phys. Commun.* at press
- [17] Gabathuler J P and Steeb S 1979 *Z. Naturf. a* **34** 1314
- [18] Li X P, Allen P W, Car R and Parrinello M 1989 *Bull. Am. Phys. Soc.* **34** 410
- [19] Bellissent R, Bergman C, Ceolin R and Gaspard J P 1987 *Phys. Rev. Lett.* **59** 661
- [20] Menelle A, Bellissent R and Flank A M, 1987 *Europhys. Lett.* **4** 705
- [21] Jank W *Thesis, Technische Universität Wien* (unpublished)  
Jank W and Hafner J *Phys. Rev. B* at press
- [22] Indlekofer G, Oelhafen P, Lapka R and Güntherodt H J 1988 *Z. Phys. Chem.* **157** 465
- [23] Shevchik N J, Tejada J, Cardona M and Langer D W 1973 *Solid State Commun.* **12** 1285
- [24] Schlüter M, Joannopoulos J D, Cohen M L, Ley L, Kowalczyk S, Pollak R and Shirley D A 1974 *Solid State Commun.* **15** 1007
- [25] Waseda Y 1980 *The Structure of Non-Crystalline Materials* (New York: McGraw-Hill)